Journal of
Water & Climate Change

IWA PUBLISHING

Journal of Water and Climate Change Vol 15 No 9, 4596 doi: 10.2166/wcc.2024.207

Regional power duration curve model for ungauged intermittent river basins

Turan Alakbar and Halil Ibrahim Burgan*
Department of Civil Engineering, Akdeniz University, Antalya, Turkey
*Corresponding author. E-mail: burgan@akdeniz.edu.tr

TA, 0009-0000-3149-6211; HIB, 0000-0001-6018-3521

ABSTRACT

Hydropower is a sustainable and renewable energy source that can serve as a practical and economically viable solution to the future possible energy crisis and climate change scenarios. Moreover, it possesses a higher energy density compared to other alternative renewable energy sources such as solar, wind energy, etc. In order to determine the potential of hydropower, long-term observed hydrometeorological data of streamflow, precipitation, etc. are crucial. This study investigates a new power duration curve (PDC) methodology. Basin characteristics such as drainage area and basin relief with meteorological data as precipitation are used for regional models in the application. The classification based on geographical locations is made for regional models. Six models based on equation type were utilized to determine the optimal regional model. Absolute errors of cease-to-flow point estimates ranging from 0.01 to 11.49% were observed. The model provided successful results according to Nash–Sutcliffe efficiency which is widely used in hydrological studies very close to 1 and higher than 0.87 except for one streamflow gauging station therewithal all other calculated performance metrics. It is observed that power and cease-to-flow point estimates of intermittent rivers can be obtained with a new PDC model based on basin characteristics.

Key words: hydropower, intermittent river, power duration curve, regional model

HIGHLIGHTS

- A novel approach for the power duration curve estimation.
- Forecasting hydropower potential in intermittent rivers.
- Regressional models based on basin characteristics.

INTRODUCTION

Water is a crucial resource in energy production and environmental activities. All civilizations need energy services for basic human needs and production processes. Hydropower as a renewable energy source is considered cleaner than fossil fuels, but it still has negative environmental effects. These include disrupting ecosystems, causing habitat loss, blocking migration routes for fish, altering river dynamics, emitting methane, risking dam failures and impacting communities and cultural heritage. Dams can block critical fish migration routes between the river's downstream floodplains and upstream tributaries (Ziv *et al.* 2012). The temporary introduction of methylmercury into the food chain needs to be monitored/managed (Yuksel 2010). These negative impacts can be kept to a minimum thanks to the planned and optimal water resources management in river basins. In recent years, the rise in the global population has led to a higher demand for electricity, particularly in developing countries. Many countries possess a plentiful potential for hydropower that has yet to be researched. Therefore, energy requirements necessitate a shift towards clean energy sources with limited resources. Hydropower emerges as a suitable solution for mitigating the potential global energy shortage in the future (Fearnside and Pueyo 2012; Valero 2012).

Currently, hydropower generation has emerged as the leading source of clean energy production, considering the increasing incidence of droughts and floods. The dams and other hydraulic structures constructed to support the generation of electricity also serve purposes such as agricultural irrigation, the provision of potable water and reservoir protection. In recent years, there has been an increase in the prominence of hydropower generation due to concerns about carbon emissions from burning fossil fuels and the potential environmental risks associated with nuclear power plants. To identify renewable energy sources and optimize their utilization, it is necessary to first predict the available resources for the given

application. Hydropower is widely considered a significant potential energy source globally. Hydropower, the focus of this study, can be harnessed by directly converting the kinetic energy of water into electricity or by initially transforming the potential energy of water into kinetic energy before converting it into electrical energy. The energy demand necessitates the exploration of clean energy sources within limited resources. Therefore, it is paramount to comprehend the potential of hydropower in rivers, a source of clean energy. A plethora of studies exist examining this potential in the literature. It is necessary to analyze a river's flow characteristics within a hydrologic basin in a given year or over a long period to determine its hydropower capacity. For this analytical process, power duration curves (PDCs) are commonly employed. However, since the flow characteristics of an intermittent river vary from year to year or even seasonally, it is difficult to estimate the PDC of the river. Hence, to calculate the hydroelectric power potential of intermittent river basins without measured streamflow data, there is a need to create PDCs (Yuksel 2010; Huxter & Van Meerveld 2012; Arthur *et al.* 2020).

The literature has some studies based on different methodologies to estimate flow and PDCs at a regional scale. For example, a hydrological model can be developed using hourly time-series data. Hourly rainfall, temperature and flow values of the river basin were used for the analysis of the hydrological processes. By creating a PDC, the energy potential of the basin was determined (Fujimura *et al.* 2014). The soil and water assessment tool (SWAT) model was used in the studies based on hydropower potential in river basins (de Oliveira *et al.* 2017; Thin *et al.* 2020; Yankey *et al.* 2023). The Distributed Hydrological Model of the National Institute for Space Research (MHD-INPE) hydrological model was applied to evaluate the effects of climate change on energy production (Mohor *et al.* 2015). Furthermore, different models as exponential and power models were used to derive regional flow duration curves (FDCs; Quimpo *et al.* 1983). In addition, a study identified the cubic model as the most appropriate based on the findings (Mimikou & Kaemaki 1985). A regional-scale application of the index-flow model was carried out to create long-term annual FDCs (Castellarin *et al.* 2007). In another study aimed at obtaining FDCs for ungauged basins, a semi-parametric model referred to as the index model was employed (Li *et al.* 2010). Log-logistic and generalized Pareto distribution (Castellarin *et al.* 2004), polynomial method and area index method (Yu *et al.* 2002), three-dimensional Kriging interpolation method (Castellarin 2014) and stepwise multiple linear regression were used to obtain regional FDCs (Boscarello *et al.* 2016). In ungauged tributary streams, multivariate adaptive regression spline and random forest methods were used to obtain FDCs (Vaheddoost *et al.* 2023). A regression equation that takes drainage area and annual precipitation as input was used to derive the annual FDC model (Burgan & Aksoy 2018) and the previous study was extended to the monthly FDC model (Burgan & Aksoy 2020). Soft computational techniques such as artificial neural networks and gene expression programming methods were also applied (Hashmi & Shamseldin 2014; Bozchaloei & Vafakhah 2015). Moreover, five parametric and two statistical models (Mendicino & Senatore 2013), stochastic index method (Rianna *et al.* 2013), Burr XII probability distribution (Costa *et al.* 2014), normalized nondimensional daily streamflow model (Burgan & Aksoy 2022) and evolutionary polynomial regression were used to obtain FDCs of intermittent rivers (Costa *et al.* 2020).

Only drainage areas of river basins were utilized at the very beginning of regional model studies on this subject (Singh 1971; 2001). In this study, basin relief, precipitation and combinations of these parameters were used in addition to the drainage area to keep the model practical and make more accurate predictions. Franchini & Suppo (1996) proposed to use an exponential model and Rojanamon *et al.* (2007) used logarithmic, quadratic, cubic, power and exponential models for FDCs. A polynomial model has also been tried to determine the cease-to-flow points and hydropower potential of intermittent rivers in this study in addition to previous models. Rospriandana & Fujii (2017) combined geographic information system methods with the SWAT in order to assess small hydropower potential and similarly, theoretical hydropower potential has been evaluated by Guiamel & Lee (2020) using the SWAT hydrological model. Jung *et al.* (2021) used the Kajiyama formula, modified two-parameter monthly (TPM), tank model and four blending techniques for the estimation of the hydropower potential in ungauged basins.

Although the hydropower potential of rivers has been determined using different methods in the literature, intermittent rivers and cease-to-flow points have not been considered in previous studies. The motivation of this study is based on research on hydropower potential in intermittent rivers. It is known that FDCs in intermittent rivers have a significant inter-annual variability (Figure 1). The year-to-year variability of an intermittent river numbered D09A057, located in the Antalya basin and with a drainage area of 185 km^2, between 2006 and 2015 is given in Figure 1. The intermittent river numbered D09A057 was chosen because it showed similar intermittency characteristics and FDCs with other rivers. Flow duration curves are very sensitive to basin characteristics and meteorological components in small river basins. There are difficulties with two main estimations for ungauged intermittent rivers in the problem: streamflow and cease-to-flow point on the PDC.

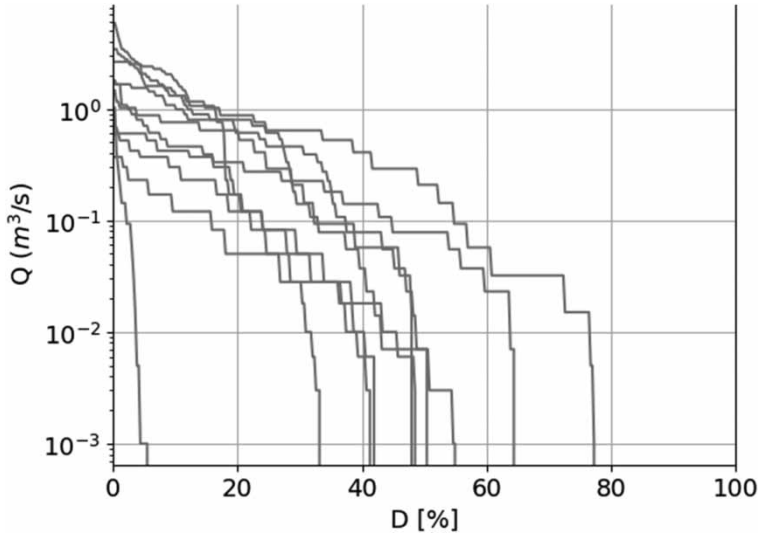

Figure 1 | Between-year variability of FDCs.

It can be challenging to estimate the FDC and streamflow of intermittent rivers, which makes it hard to determine their hydropower potential. Additionally, sufficient observation length in the basin without interruption may not always be feasible. Even considering the tributaries in the river, observation periods may still be shorter. There is a lack of research on the FDC in intermittent rivers and no research has been carried out on the PDC in intermittent rivers. In previous studies, the PDC in intermittent (zero-flow) rivers has not been taken into account. The PDC can be utilized in the proposed model and extensive project work, including hydropower plants. The model presented here has practical data availability, enabling its implementation in any region or river basin.

The purpose of this study is to determine the hydropower potential of intermittent rivers by utilizing a new regional PDC model. The regional model for the Antalya Basin, Turkey is based on drainage area and basin relief values from streamflow gauging stations, along with precipitation values from CHRS RainSphere remote sensing data. The topographical and meteorological variables in the Antalya Basin are analyzed with regression techniques to identify the best-fit model for small catchments.

STUDY AREA AND DATA

The Antalya basin is selected for the case study in order to identify the PDC of intermittent rivers. The average monthly temperature of the hottest month of the basin on the coast is 28.2°C (Antalya); the temperature in the interior is about 5°C lower. The coldest winter month averages 9.9°C on the coast, while in the interior the temperature drops to 0.5°C. When the precipitation distribution of the Antalya Basin is analyzed, it is seen that the least precipitation falls to the west and north, while the most precipitation falls to the east and south. The average annual precipitation, which is around 1,000 mm in the south, drops to 600 mm in the north. Approximately 200 km in length and 170 km in width, the narrowest part of the basin is in the east–west direction, within the borders of Eğirdir district of Isparta province and its width is approximately 30 km. On average, 78% of Antalya province is mountainous, 10% is plain and 12% is hilly. The Antalya Basin constitutes 6.97% of Turkey's surface water potential with a 19,577 km^2 total drainage area (General Directorate of Water Management 2016, 2018).

The total precipitation decrease in the Antalya Basin over 30 years is −29.36 mm. Considering the decrease in precipitation, it can be said that climate change is effective in the Antalya Basin in general. Little research has been done on the effects of climate change on groundwater in the Antalya Basin. Under certain conditions, changes in river flows and thus the phases affecting groundwater levels are much stronger than changes in groundwater recharge. It is thought that such a situation may be the case for the Antalya Basin. Regarding groundwater quality, climate change may have a strong impact on coastal saltwater intrusion and also on groundwater salinization. In addition to seawater level rise, any increase in groundwater recharge affects the location of the freshwater/saltwater interface, and brine mixing is expected to increase as

groundwater recharge decreases. This can occur inland, where salt water settles right next to or below fresh water. Decreases in precipitation may cause the groundwater quality to decrease by becoming salinized (General Directorate of Water Management 2016, 2018).

Streamflow, drainage area, basin relief and precipitation data are used for the application of the study. Precipitation values are obtained from CHRS RainSphere data and other values are produced from topography. Daily streamflow data of the gauging stations located in the Antalya basin are taken into consideration. The streamflow data are obtained from the General Directorate of State Hydraulic Works, Turkey (DSI, *the abbreviation of Devlet Su İşleri in Turkish*). First of all, an inventory study of streamflow gauging stations was conducted for the evaluation of each basin from 1964 to 2015. The missing data in a year are determined for the observation period of the streamflow gauging stations. The years with complete observations without any missing daily data are considered in the study. Detailed information about data observations is provided in Supplementary material (Figure SM1). A colorless box means no data, a yellow box means that there is missing data and a green box means that there are 365-daily data. The observation period is considered from 1964 to 2015. A total of 11 streamflow gauging stations with a drainage area larger than 10 km^2 are used in the regional PDC model application. The geodetic locations of the stations used in the study are given in Table 1 and their locations on a map with basin boundary are given in Figure 2. The flows greater than zero (cease-to-flow point) of the gauging stations are presented in Table 2. Then, the homogeneity test of used monthly streamflow data is provided in Figure 3. The streamflow gauging stations have a common streamflow observation period from 2000 to 2015. Therefore, a monthly homogeneity test was produced using the dataset observed for these years.

The drainage area and basin relief values of the gauging stations are obtained from basin topography. The drainage area and basin relief values of the gauging stations are presented in Table 2. The gauging stations in Table 2 are located on the only tributaries of the rivers, not the main rivers. CHRS RainSphere is a climate data discovery tool specifically designed to encourage the independent conduct of climate studies. It provides high-resolution spatial and temporal information on precipitation patterns, which is essential for understanding and predicting weather and climate phenomena. The average annual precipitation data of intermittent river basins at the validation stage between 1983 and 2021 are presented in Figure 4 and Table 3. The Mann-Kendall (MK) trend test is one of the most widely used trend detection methods. Being rank-based, the MK trend test is unaffected by the actual distribution of the data even when significantly skewed with some outliers, making it quite suitable for hydrological data (Burgan *et al.* 2013; Hu *et al.* 2020). The average annual precipitation data of intermittent river basins at the calibration stage are presented in the Supplementary material (Figure SM2). Then, an isohyetal map of mean annual precipitation data is provided in Figure 5.

PDC MODEL

Steps of the model

This study presents a regional model for determining the hydropower potential of intermittent rivers by using a new regional PDC model. The following flow diagram has been developed for this purpose (Figure 6). The model application steps are

Table 1 | Coordinates of streamflow gauging stations

SGS number	Station name	River name	Lon (N)	Lat (E)
D09A031	Kapuz Boğazı	Karaman Çayı	36.93	30.57
D09A057	Gökçali	Hoyran Deresi	38.30	30.95
D09A060	Göl Giriş	Çaydere Gölü	37.84	30.90
D09A075	Avşar Köprüsü	Gelendost Deresi	38.13	30.99
D09A086	Belence	Aksu Deresi	37.62	31.12
D09A104	Ahırtaş	Beyhasan Deresi	37.20	30.73
D09A106	Hacıbekar	Göldere	37.33	30.19
D09A111	Doyran	Doyran Deresi	36.89	30.51
D09A114	Yavrudoğan	Kızıllar Deresi	36.89	31.31
D09A116	Şişeler Köyü	Naras Deresi	36.87	31.40
D09A125	Küçükköy	Kurupınar Deresi	37.11	30.30

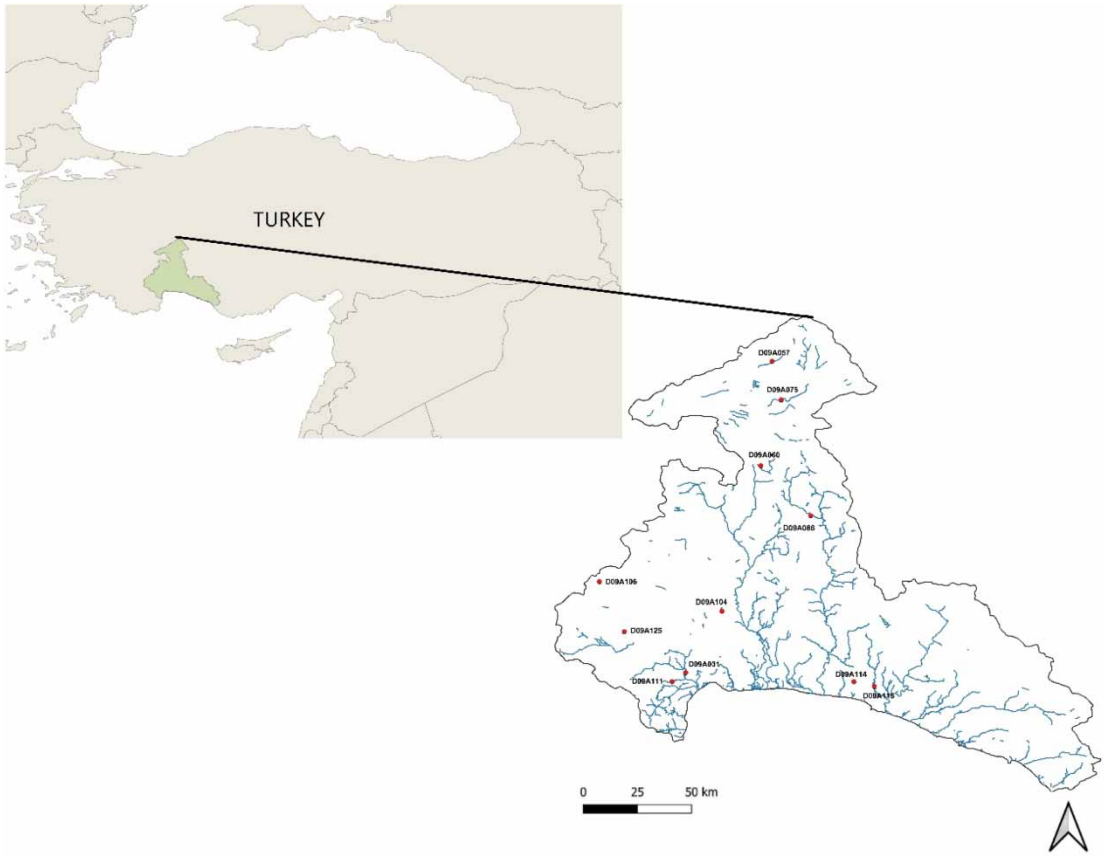

Figure 2 | Location map of streamflow gauging stations.

detailed below. These steps enable the calculation of hydropower potential in an ungauged intermittent river basin that has no streamflow data. The evaluation criteria employed to assess the model results are subsequently delineated in this section.

(a) Selection of intermittent rivers in the basin: Gauging stations with observation periods of 10 years or more should be selected to be able to assess long enough duration not affected by dry and wet periods. At the validation stage, the variables (as drainage area and precipitation) of the selected gauging stations should fall within the smallest and largest ranges of the

Table 2 | Statistical and physical characteristics of the streamflow gauging stations (C_V: coefficient of variation, C_S: coefficient of skewness, IR: intermittency ratio, A: drainage area, H: basin relief)

SGS number	Average (m^3/s)	Min (m^3/s)	Max (m^3/s)	St. Dev. (m^3/s)	C_v	C_s	IR (%)	A (km^2)	H (m)
D09A031	1.37	0.00	150	4.91	3.58	0.63	63.50	404.60	52
D09A057	0.26		8.33	0.54	2.13	1.37	52.13	185	950
D09A060	2.64		32.60	3.26	1.24	1.32	82.99	111.20	935
D09A075	1.53		76.30	3.48	2.27	1.02	71.68	989	940
D09A086	5.09		362	14.43	2.84	0.82	98.72	349	1000
D09A104	0.10		13.30	0.44	4.23	0.61	62.18	12.75	403
D09A106	0.07		4.10	0.22	3.01	0.79	85.15	32.21	1002
D09A111	0.75		37.10	1.30	1.73	1.10	96.67	105.80	145
D09A114	0.26		39.60	1.05	4.07	0.70	63.80	22.54	75
D09A116	4.30		344	14.57	3.39	0.78	74.08	193.90	30
D09A125	0.006		0.22	0.011	1.88	1.03	59.98	11.60	890

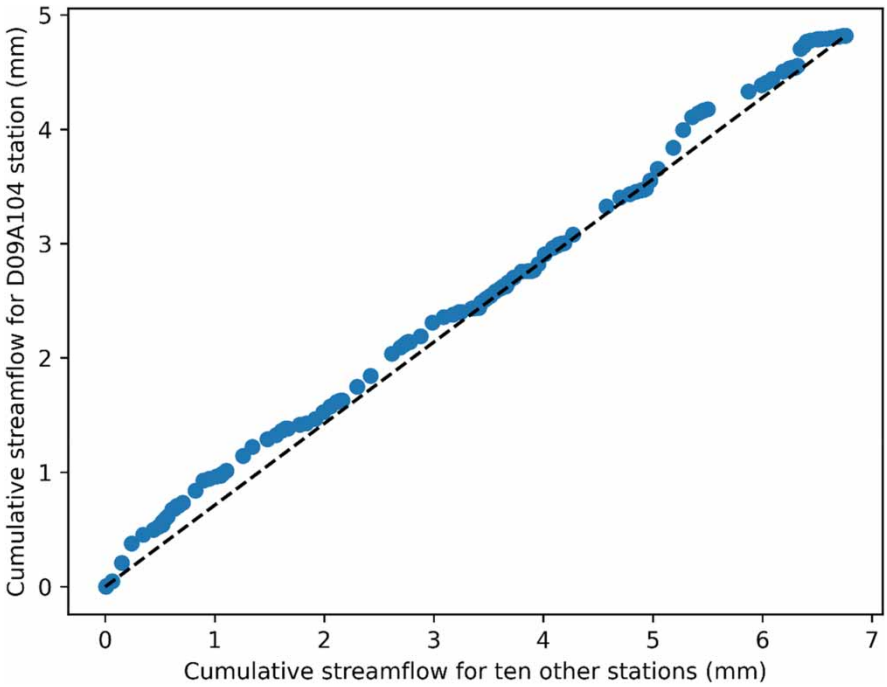

Figure 3 | Double mass curve for homogeneity test of streamflow data.

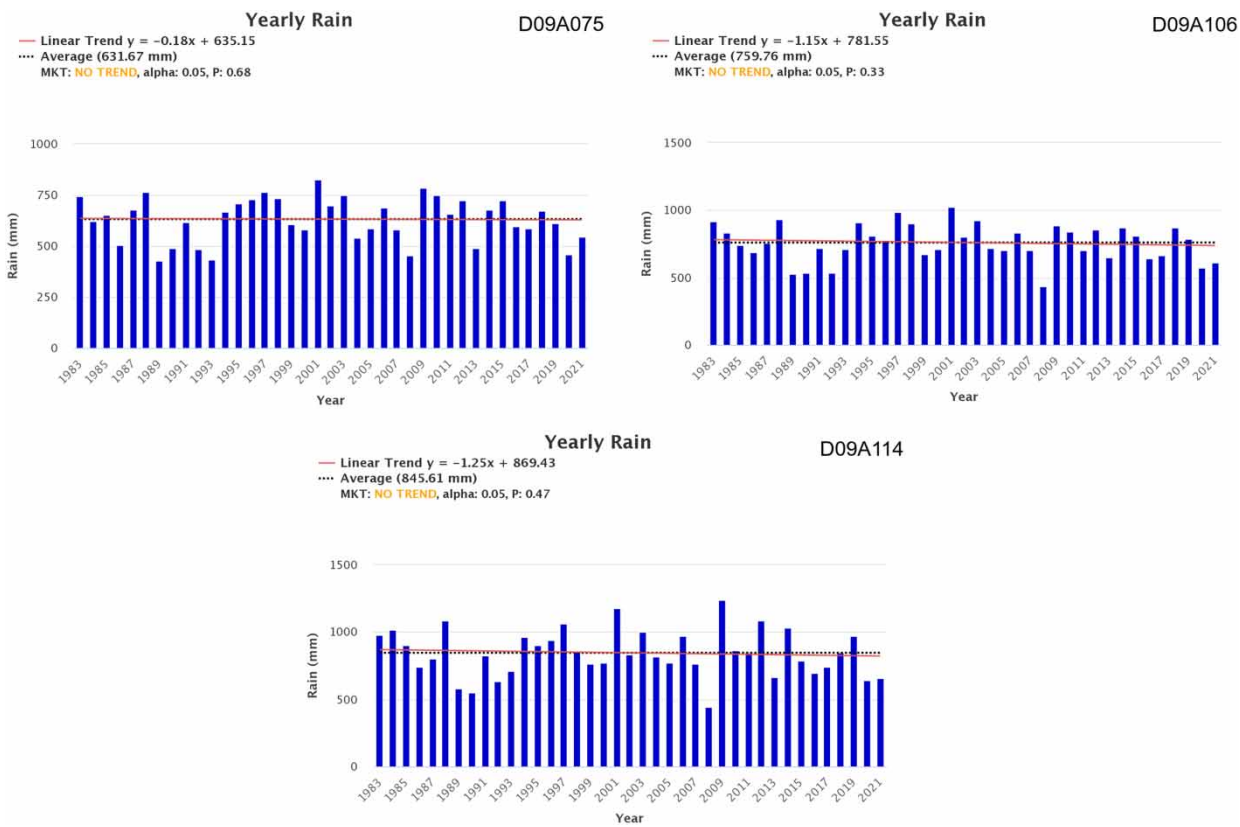

Figure 4 | Annual average precipitation data of streamflow gauging stations at the validation stage.

Table 3 | Mann–Kendall trend test results

SGS	Trend	Alpha	*p*
D09A031	No Trend	0.05	0.22
D09A057			0.73
D09A060			0.81
D09A075			0.68
D09A086			0.68
D09A104			0.18
D09A106			0.33
D09A111			0.40
D09A114			0.47
D09A116			0.47
D09A125			0.22

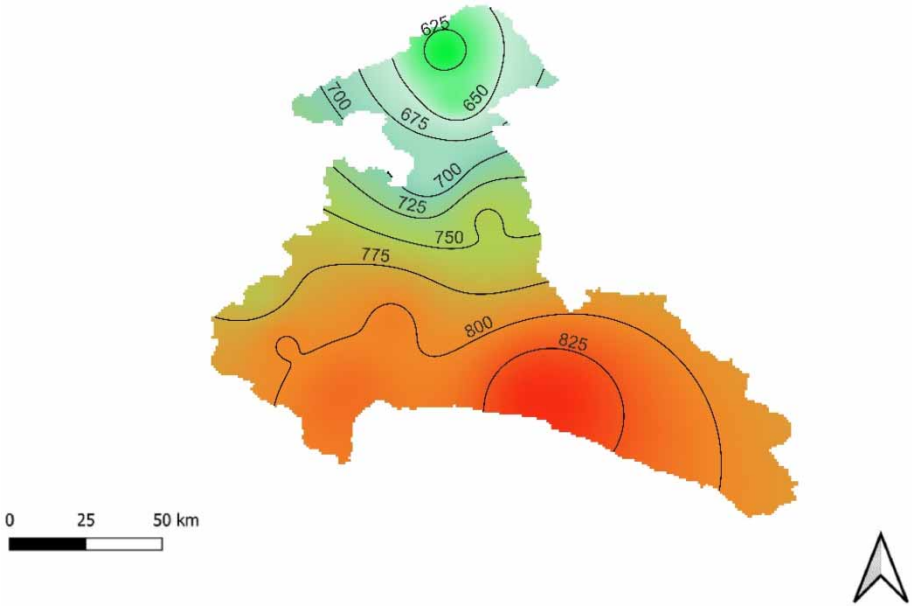

Figure 5 | Isohyetal map of mean annual precipitation data in the Antalya Basin.

variable values of the stations identified during the calibration stage. Therefore, the selection of calibration and validation stations is based on the cease-to-flow point and basin characteristics to provide this requirement.

(b) Daily streamflow data from selected gauging stations and other variables: The streamflow data are obtained from relevant institutions through streamflow monitoring yearbooks or downloadable from their websites. The basin characteristics can be calculated from topographical data. Then, precipitation data can be acquired from the CHRS RainSphere dataset as remote sensing products.

(c) Statistical analysis of streamflow data: For the statistical analysis of streamflow data, mean streamflow values and percentages of streamflows greater than zero (cease-to-flow point) are computed. The mean streamflow values are obtained by calculating the average daily streamflow data during the observation period of each gauging station. The cease-to-flow points of the gauging stations are obtained by dividing the number of streamflows greater than zero by the number of streamflows equal to zero.

(d) Flow and PDCs of intermittent rivers (observation): Flow duration curves are derived using daily flow data collected during the observation period of the gauging stations. The flow and PDCs are derived using a new Python code in

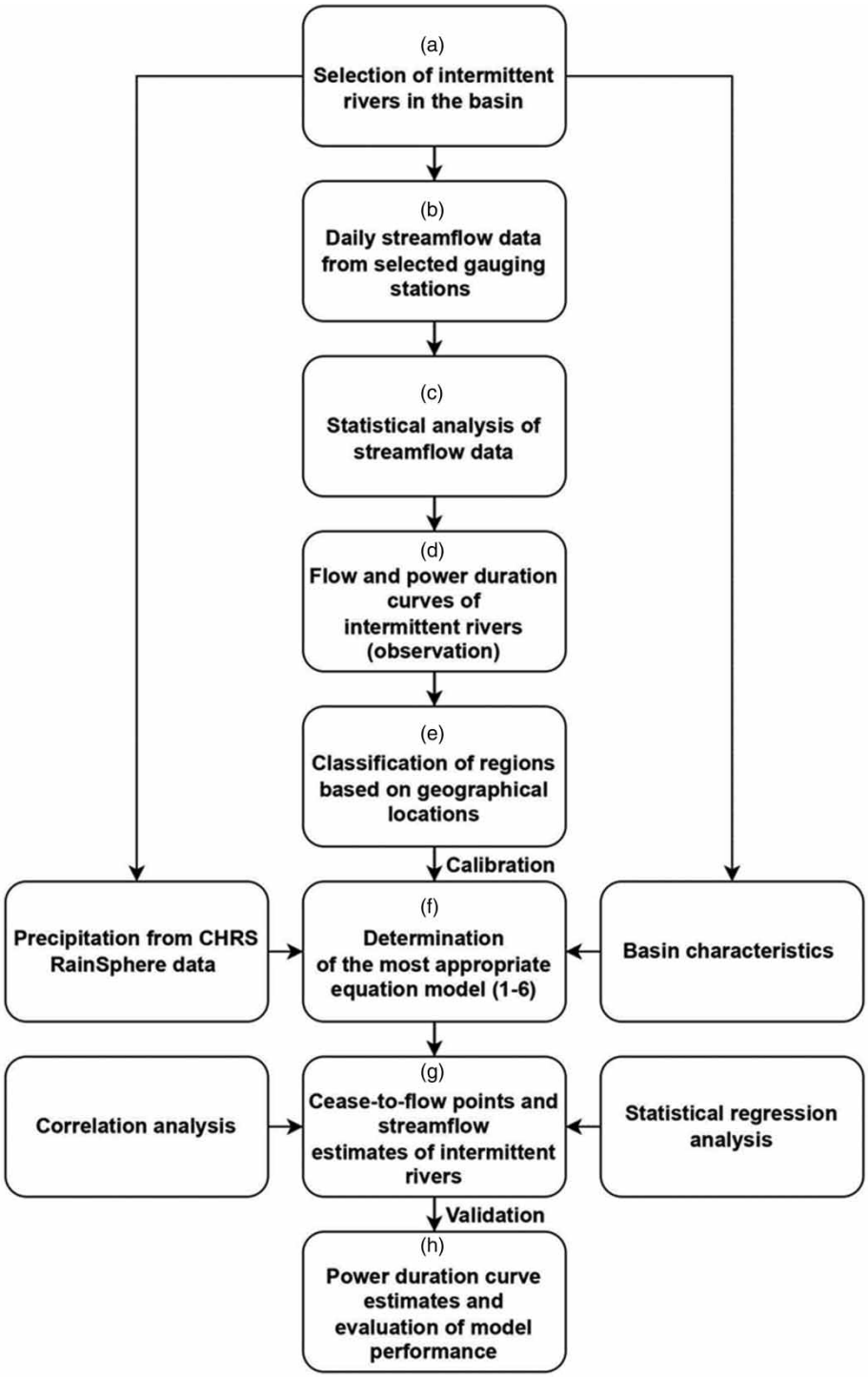

Figure 6 | Steps of the model.

Figure SM3. PDCs are derived by applying the water power Equation (1) to the FDCs of the gauging stations.

$$P = \gamma.Q.H.\eta_t \tag{1}$$

where hydropower P (kW), specific weight of water γ (N/m^3), discharge Q (m^3/s) and differential water head H (m) and synthesis efficiency coefficient η_t. The PDCs obtained at this stage are compared with the PDC estimates obtained in the following steps.

(e) Classification of regions based on geographical locations: For the regional PDC model, regional classification as North, Southeast, Southwest, etc. can be made considering geographical locations of intermittent river basins.
(f) Determination of the most appropriate equation Models (1–6): To determine the most suitable equation model for the cease-to-flow point, the determination coefficients (R^2) of the calibration stations are calculated. Subsequently, the absolute errors of the cease-to-flow point for the calibration stations are acquired to identify the best model among the determined equation models.
(g) Cease-to-flow points and streamflow estimates of intermittent rivers: Correlation analyses are used to establish the relationship between the equation model and basin characteristics. Subsequently, statistical regression analyses are used to obtain the cease-to-flow point estimates of gauging stations. The most appropriate equation model is used to generate an estimation of high, medium and low flow after estimation of cease-to-flow points. The most appropriate equation model for flow predictions is identified based on BiasPHV, SPDC and BiasPLV criteria.
(h) PDC estimates and evaluation of model performance: PDCs are created after calculating the cease-to-flow point estimates of each station. The evaluation criteria R^2, Nash–Sutcliffe efficiency (NSE), mean absolute error (MAE), root mean squared error (RMSE), mean squared error (MSE), volume error (VE), percent bias in PDC high-segment volume (BiasPHV), the slope of PDC (SPDC) and percent bias in PDC low-segment volume (BiasPLV) are used to evaluate the performance of regional PDCs.

Performance metrics

The metrics listed in Table 4 are used to check the performance of the proposed PDC model. A single evaluation criterion is inadequate to assess high and low power values on the PDC. Therefore, a more appropriate approach is to evaluate and interpret the PDC by dividing it into sections. In the expressions of the performance criteria in Table 4, the following notations were applied: RSS: sum of squared residuals, TSS: total sum of squares, P_i: observed power value at rank i, $\tilde{P}_i$: power

Table 4 | Performance metrics

Metrics	Expression	Range	Remarks
Coefficient of determination	$R^2 = \frac{\text{RSS}}{\text{TSS}}$	$0 \le R^2 \le 1$	R^2 approaching 1 is better.
Nash–Sutcliffe efficiency	$\text{NSE} = 1 - \frac{\sum_{i=1}^{N}(\tilde{P}_i - P_i)^2}{\sum_{i=1}^{N}(P_i - \bar{P})^2}$	$-\infty \le \text{NSE} \le 1$	NSE approaching 1 is better.
Mean absolute error	$\text{MAE} = \frac{1}{N}\sum_{i=1}^{N}\lvert\tilde{P}_i - P_i\rvert$	$0 \le \text{MAE} \le \infty$	MAE approaching zero is better.
Root mean square error	$\text{RMSE} = \sqrt{\frac{1}{N}\sum_{i=1}^{N}(\tilde{P}_i - P_i)^2}$	$0 \le \text{RMSE} \le \infty$	RMSE is dimensional as the variable. RMSE approaching zero is better.
Mean square error	$\text{MSE} = \frac{1}{N}\sum_{i=1}^{N}(\tilde{P}_i - P_i)^2$	$0 \le \text{MSE} \le \infty$	MSE approaching zero is better.
Volume error	$\text{VE} = \frac{\sum_{i=1}^{N}\tilde{P}_i - \sum_{i=1}^{N}P_i}{\sum_{i=1}^{N}P_i}$	$-\infty \le \text{VE} \le \infty$	VE approaching zero is better.
Percent bias in PDC high-segment volume	$\text{BiasPHV} = \frac{\sum_{i=1}^{N}(\tilde{P}_i - P_i)*100}{\sum_{i=1}^{N}P_i}$	$0 \le \text{BiasPHV} \le 100$	BiasPHV is used for the higher part of PDC (the highest 20%)
Slope of PDC	$\text{SPDC} = \frac{[\log(P_{m1}) - \log(P_{m2})] - [\log(P_{o1}) - \log(P_{o2})]}{[\log(P_{o1}) - \log(P_{o2})]}*100$	$0 \le \text{SPDC} \le 100$	SPDC is used for the medium part of PDC (from 20–70%)
Percent bias in PDC low-segment volume	$\text{BiasPLV} = \frac{\sum_{i=1}^{N}(\tilde{P}_i - P_i)*100}{\sum_{i=1}^{N}P_i}$	$0 \le \text{BiasPLV} \le 100$	BiasPLV is used for the lower part of PDC (the lowest 30%)
Absolute error	$\varepsilon = \lvert\tilde{P}_i - P_i\rvert$	$0 \le \varepsilon \le \infty$	ε approaching zero is better.

value calculated from the model at rank i, $\bar{P}$: observed average power value for many years, P_{o1}: power value observed at 20% exceedance probability, P_{o2}: power value observed at 70% exceedance probability, P_{m1}: power value calculated from the model at 20% exceedance probability and P_{m2}: power value calculated from the model at 70% exceedance probability.

RESULTS

In an effort to identify the optimal equation model for estimating the cease-to-flow point of intermittent rivers situated in the North, Southwest and Southeast regions of the Antalya Basin, the determination coefficients (R^2) of the calibration stations were calculated. Three equation models were selected for each region based on the highest average R^2 (Table 5). Model (6) cannot be used for estimating the cease-to-flow point, as it is the only selected model among the three that is an exponential equation (Table 6). To determine the best model among the selected equation models, the absolute errors of the cease-to-flow points of the calibration stations were obtained (Table 7). The calculations revealed that the best equation model for all regions is Model (2).

After the flow estimates of the gauging stations are calculated, PDCs are obtained by applying the water power Equation (1) to the FDC. The PDCs are presented in Figure 7 and Figure SM4, respectively at the validation and calibration stages.

Table 5 | R^2 values of Models (1–6)

MODEL							
Region	**SGS**	**(1)**	**(2)**	**(3)**	**(4)**	**(5)**	**(6)**
North	D09A060	0.996	0.998	0.989	0.871	0.798	0.955
	D09A086	0.822	0.932	0.862	0.548	0.996	0.940
	D09A057	0.981	0.996	0.984	0.822	0.941	0.982
	Average	0.933	***0.975***	***0.945***	0.747	0.912	***0.959***
Southwest	D09A125	0.937	0.957	0.971	0.861	0.886	0.951
	D09A111	0.931	0.980	0.951	0.691	0.929	0.990
	D09A031	0.922	0.974	0.962	0.760	0.969	0.968
	Average	0.930	***0.970***	***0.961***	0.771	0.928	***0.970***
Southeast	D09A104	0.938	0.976	0.969	0.775	0.960	0.983
	D09A116	0.849	0.950	0.866	0.576	0.998	0.977
	Average	0.894	***0.963***	0.918	0.676	***0.979***	***0.980***

Table 6 | Equations of Models (1–6)

Model		
(1)	(2)	(3)
$y = ax^2 + bx + c$	$y = ax^3 + bx^2 + cx + d$	$y = a\ln x + b$
(4)	(5)	(6)
$y = ax + b$	$y = \frac{a}{x} + b$	$y = a.e^{bx}$

Table 7 | Absolute error values (%) of Models 2, 3 and 5

Region	Model (2)	Model (3)	Model (5)
North	**6.34**	13.92	–
Southwest	**0.79**	11.32	–
Southeast	**2.75**	–	20.80

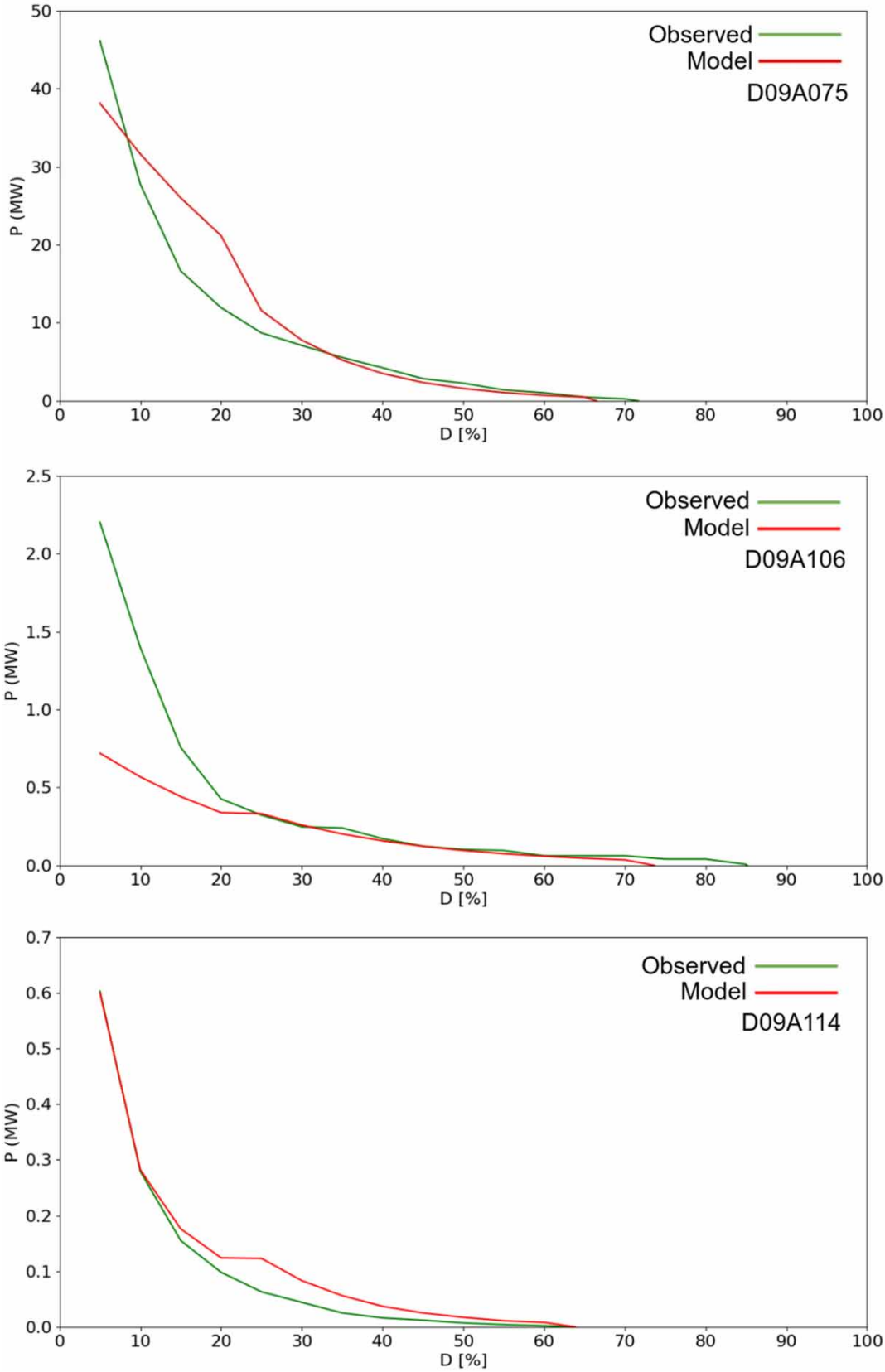

Figure 7 | PDCs of streamflow gauging stations at the validation stage.

Calculated power (MW) values are shown in Table 8, where P (MW) represents the power value and D (%) represents the percentage of exceedance (Figure 7).

The calibration results obtained from gauging station D09A060, situated in the North region, suggest that the modeled PDC is in close proximity to the observed PDC. The percentage of exceedance, which ranges from 30 to 60%, is deemed acceptable, particularly when the cease-to-flow point and the overall PDC are taken into account (Figure SM4). On the other hand, the exceedance percentages of gauging stations D09A086 (calibration) and D09A075 (validation), also located in the North region, are observed to fluctuate between 5 and 30%. It is pertinent to note that the drainage areas of these two stations are relatively vast and since there exists a correlation between the drainage area and peak flowrate, it is hypothesized that this may be the root cause of the differences observed (Figures 7 and A3). Finally, the D09A057 station produced quite commendable results, with estimates of the exceedance percentage ranging between 5 and 20%. Only marginal disparities are identified between 20 and 40% (Figure SM4).

It has been noted that the most significant disparities between the modeled and observed values at gauging station D09A125 (calibration), located in the Southwest region, occur within the 25–35% range of exceedance percentages. Within this range, the modeled power values are smaller than the observed values, as illustrated in Figure SM4. On the other hand, gauging station D09A111 (calibration) expresses opposite results, wherein the modeled power values are greater than the observed values within the range of 10–25% exceedance percentage, but the opposite trend is evident after the 30% exceedance percentage, as indicated in Figure SM4. D09A031 (calibration), an intermittent river with the largest drainage area of 404.60 km^2 within the Antalya basin, exhibits minimal discrepancies between the modeled and observed values in the range of 20–30% exceedance percentage, although variances are manifest in other exceedance percentages, as demonstrated in Figure SM4. Assessment of station D09A106 (validation) exposes adequate predictions at mid and low power values, with differences arising only at peak power values (exceedance percentage ranging between 5 and 25%), as delineated in Figure 7.

At gauging station D09A104 (calibration), situated in the southeastern region, the modeled power values demonstrate a smaller magnitude in comparison to the observed power values beyond the 10% exceedance threshold (Figure SM4). Conversely, gauging station D09A114 (validation) presents an opposing observation where the modeled power values are greater than the observed values (Figure 7). An analysis of gauging station D09A116 (calibration), the location with the largest drainage area in the region, indicates that the observed and modeled values are closely aligned across all levels of exceedance (Figure SM4). The computed power (MW) values derived from the PDC of gauging stations with observation periods ranging between 10 and 25 years reveal that the observed and modeled values exhibit a similar magnitude in proximity to each other (Table 8).

Table 8 | Annual total power (MW) values of streamflow gauging stations

SGS	Region	Power (Observed)	Power (Model)	A (km^2)	N (Year)
Calibration					
D09A060	North	66.49	61.27	111.20	20
D09A086		72.74	80.42	349	25
D09A057		5.25	5.03	185	19
D09A125	Southwest	0.20	0.20	11.60	11
D09A111		2.53	2.51	105.80	21
D09A031		1.92	1.93	404.60	13
D09A104	Southeast	0.59	0.52	12.75	23
D09A116		2.86	2.76	193.90	13
Validation					
D09A075	North	25.73	30	989	22
D09A106	Southwest	2.63	1.55	32.21	10
D09A114	Southeast	0.31	0.39	22.54	16

DISCUSSION

Climate change can complicate the estimation of cease-to-flow points in intermittent rivers. Changing precipitation patterns and increased temperatures can alter the flow regime and lead to more frequent and prolonged dry periods. These changes can make historical data less reliable and introduce uncertainties into streamflow predictions, making it harder to estimate when the river will cease to flow. Future climate scenarios indicate that there will be a growing impact of droughts on various economic sectors, particularly in developing countries in the southern and eastern Mediterranean (Tramblay *et al.* 2020). For this reason, climate change scenarios provide the basis for policy decision-making and strategy development for climate change mitigation and adaptation (Selek *et al.* 2016).

The cease-to-flow point of an intermittent river varies from year to year and the cease-to-flow points vary greatly at the streamflow gauging stations located in different river branches within the same basin. Due to this variability, estimating the cease-to-flow point in rivers is not easy. There are limited studies on the subject in the literature and it has been observed that in these studies, gauging stations are classified and regional models are developed for each geographical region. In this study, the Antalya basin is divided into three geographical regions: North, Southwest and Southeast, and regional models are developed. The cease-to-flow points of all intermittent rivers in the Antalya basin are calculated using Model (2) and regression analysis. In the regional model study, each variable in the basin is examined by correlation analysis. Accordingly, variables that are found to have a high correlation with each other are identified by correlation analysis and related variables are excluded from the model to ensure the neutrality of models. While selecting the appropriate variables for regression models in each region, basin-variable combinations are evaluated. The model correctly predicts the cease-to-flow points of gauging stations. Absolute errors ranging from 0.01 to 11.49% are observed as a result of the calculations. In the literature, it is stated that errors of up to 30–40% between observations and models are acceptable (Shao *et al.* 2009). Another widely used paper classified the performance metrics by usage area and it provides this acceptable range (Yilmaz *et al.* 2008; Moriasi *et al.* 2015). Additionally, to examine the performance of the equations in detail and to determine the most appropriate evaluation criterion, the determination coefficient (R^2), NSE coefficient, MAE, RMSE, MSE, VE, BiasPHV, SPDC and BiasPLV are calculated (Table 9).

The determination coefficient values (R^2) of calibration gauging stations range from 0.95 to 0.99, while the R^2 values of validation gauging stations range from 0.89 to 0.99. As the calculated R^2 value approaches 1, it is understood that the predicted results from the model are closer to the observations. Therefore, it can be said that good results are obtained at the calibration and validation stations. The NSE evaluation criterion used for the assessment of high-power data, like R^2, provides good results for a value close to 1. The values of calibration gauging stations range from 0.94 to 0.99, indicating good results. The NSE value of validation gauging station D09A075 is calculated as 0.87, while the NSE value of validation gauging station D09A114 is 0.98. It is thought that successful results are obtained at these two gauging stations. However, the NSE value of validation gauging station D09A106, located only in the Southwest region, is calculated as 0.41, indicating a poor result. The performances during training and testing periods show good agreement with each other. During the training period, NSE values range between 0.917 and 0.992, while during the testing period, NSE values range between 0.931 and

Table 9 | Performance metrics for the streamflow gauging stations (colors refer to the performance of the model; green: good, yellow: adequate, red: inadequate)

Calibration										
SGS	**Region**	**R^2**	**NSE**	**MAE**	**RMSE**	**MSE**	**VE**	**BiasPHV**	**SPDC**	**BiasPLV**
D09A060	North	0.99	0.99	0.24	0.32	0.10	-0.08	-0.01	6.28	0
D09A086		0.95	0.94	0.68	1.25	1.57	0.11	5.13	23.14	-28.23
D09A057		0.99	0.99	0.03	0.04	0.001	-0.04	-0.26	4.99	0
D09A125	Southwest	0.95	0.95	0.001	0.001	0.000002	-0.01	3.33	21.75	0
D09A111		0.98	0.98	0.08	0.11	0.01	-0.01	2.89	1.29	18.97
D09A031		0.98	0.98	0.14	0.21	0.05	0.01	2.51	-18.81	0
D09A104	Southeast	0.98	0.97	0.01	0.02	0.0003	-0.12	-5.38	-22.12	0
D09A116		0.99	0.99	0.18	0.24	0.06	-0.04	-0.91	-20.91	0
Validation										
D09A075	North	0.89	0.87	0.44	0.70	0.48	0.17	14.11	18.76	0
D09A106	Southwest	0.88	0.41	0.03	0.07	0.004	-0.41	-56.72	16.67	0
D09A114	Southeast	0.99	0.98	0.04	0.05	0.003	0.23	4.09	-28.01	0

0.991 (Yilmaz *et al.* 2023). When the MAE evaluation criterion used for the overall evaluation of the PDC is examined, the calibration and validation values range from 0.001 to 0.68 and 0.03 to 0.44, respectively. MAE, which changes between $0 \leq \text{MAE} \leq \infty$, is known to provide good results as the calculated value approaches zero in predicting results from the model. Successful results are observed in the application results in the North, Southwest and Southeast regions. The VE value calculated as −0.41 for validation gauging station D09A106 is considered acceptable and it can be said that the results are successful at all other gauging stations. As with MAE, a VE value close to zero provides good results. In the BiasPHV evaluation criterion used for assessing high-power data, values calculated up to 100% are considered acceptable. When calibration gauging stations are examined, the largest error observed is −5.38, while the largest error observed in validation gauging stations is −56.72. As this study concerns the PDC, SPDC is considered the most important evaluation criterion. The calibration and validation values in each region range from 1.29 to 23.14 and −28.01 to 16.67, respectively. As with BiasPHV, the SPDC values calculated up to 100% are considered acceptable. When the BiasPLV evaluation criterion used for the assessment of low power data is examined, the BiasPLV value is calculated as −28.23 for gauging station D09A086 and 18.97 for gauging station D09A111. Although there is no error in other stations, it is thought that the errors observed in the calibration stations D09A086 and D09A111 were caused by high cease-to-flow points (Table 9). RMSE and MSE have the dimension as the variable. Directly evaluating the model using these criteria is difficult because this circumstance is tried to the data range. RMSE and MSE approaching zero show better performance (Burgan & Aksoy 2022). Performance metrics for the streamflow gauging stations are at the 5% significance level.

CONCLUSIONS

It has been observed that watershed classification is necessary to determine the cease-to-flow point and to obtain PDCs of streamflow gauging stations. It is believed that a single equation model is insufficient to represent the entire river basin. In the literature, gauging stations in any watershed are classified according to the size of the basin or the percentage of the cease-to-flow point. In this study, the gauging stations are classified into three categories based on the geographical region: North, Southwest and Southeast. As a result of the models used, very small differences ranging from 0.01 to 11.49% between observed and modeled cease-to-flow points were observed for all gauging stations. Therefore, the cease-to-flow point can be obtained from regional basin characteristics. The evaluation criteria used in the study facilitated the evaluation of PDCs. Besides the NSE value of 0.41 obtained from streamflow gauging station D09A106, the model provided successful results in all evaluation criteria. In the study, six basin parameters are used: drainage area (A), basin relief (H) and precipitation (R), as well as the ratios of these parameters (A/H), (A/R) and (H/R). These parameters are considered practical and easily obtainable. Only quadratic and linear regression analyses are used in the Antalya basin study due to the small number of intermittent rivers. Eleven intermittent rivers are observed in total. Quadratic regression analyses are used in the North and Southwest regions, where three calibration gauging stations are used, while linear regression analyses are used in the Southeast region, where only two calibration gauging stations are used. In studies to be conducted in watersheds with more intermittent rivers with a lower cease-to-flow point on the PDC, exponential, logarithmic and cubic regression analyses may also be used. When Models (1–6) used in cease-to-flow point and streamflow predictions is examined, it is observed that Model (2) provided better results than other models in cease-to-flow point predictions in all regions. While Model (2) provided better results for high-flow predictions of gauging stations in North and Southwest regions, Model (6) provided better results for mid- and low-flow predictions. Although the mid- and low-flow predictions of the Southeast region are obtained using Model (6) like in other regions, it is observed that Model (5) provided better results for high-flow predictions. There are studies on flow and PDCs, hydropower potential and regional model in the literature, but there is no study on determining hydropower potential with the regional PDC method for intermittent rivers.

Finally, the development of hydropower is an ideal alternative to reduce dependence on fossil fuels such as oil, coal and natural gas in many countries. This study is expected to assist public or commercial official institutions related to water resources management in intermittent river basins in terms of determination of hydropower potential and progress on potential water resources for hydropower. The PDC model based on different variables such as basin slope and river length can be used in combination with these parameters in intermittent rivers, which is a promising area for improvement. The proposed model is expected to be widely used due to its practicality and low number of variables in the equation, while also yielding successful results. Overall, this study enhances the understanding of hydropower potential in intermittent river basins through the development and application of a new PDC methodology tailored to data-scarce regions. This adds to the body of

knowledge on the use of PDCs in different geographical contexts and expands the applicability of such studies beyond traditional hydropower assessment methods.

ACKNOWLEDGEMENTS

This study is a part of the MSc thesis of the first author under the supervision of the second. Streamflow data are provided by State Hydraulic Works, Turkey (DSI) downloadable from (dsi.gov.tr) and precipitation data by CHRS RainSphere downloadable from (rainsphere.eng.uci.edu).

AUTHOR CONTRIBUTIONS

T.A. and H.I.B. contributed to conceptualization and methodology; participated in formal analysis and data curation; investigated the work; involved in resource preparation; and wrote the original draft and reviewed and edited the manuscript. T.A. contributed to software development and visualized the published work. H.I.B. supervised the work. All authors have read and agreed to the published version of the manuscript.

DATA AVAILABILITY STATEMENT

All relevant data are included in the paper or its Supplementary Information.

CONFLICT OF INTEREST

The authors declare there is no conflict.

REFERENCES

Arthur, E., Anyemedu, F. O. K., Gyamfi, C., Tannor, P. A., Adjei, K. A., Anornu, G. K. & Odai, S. N. 2020 Potential for small hydropower development in the Lower Pra River Basin, Ghana. *Journal of Hydrology: Regional Studies* **32**, 100757. doi:10.1016/j.ejrh.2020.100757.

Boscarello, L., Ravazzani, G., Cislaghi, A. & Mancini, M. 2016 Regionalization of flow-duration curves through catchment classification with streamflow signatures and physiographic–climate indices. *Journal of Hydrologic Engineering* **21**. doi:10.1061/(asce)he.1943-5584.0001307.

Bozchaloei, S. K. & Vafakhah, M. 2015 Regional analysis of flow duration curves using adaptive neuro-fuzzy inference system. *Journal of Hydrologic Engineering* **20**. doi:10.1061/(asce)he.1943-5584.0001243.

Burgan, H. I. & Aksoy, H. 2018 Annual flow duration curve model for ungauged basins. *Hydrology Research* **49**, 1684–1695. doi:10.2166/nh.2018.109.

Burgan, H. I. & Aksoy, H. 2020 Monthly flow duration curve model for ungauged river basins. *Water (Switzerland)* **12**. doi:10.3390/w12020338.

Burgan, H. I. & Aksoy, H. 2022 Daily flow duration curve model for ungauged intermittent subbasins of gauged rivers. *Journal of Hydrology* **604**. doi:10.1016/j.jhydrol.2021.127249.

Burgan, H. I., Icaga, Y., Bostanoglu, Y. & Kilit, M. 2013 Water quality tendency of Akarcay River between 2006–2011. *Pamukkale University Journal of Engineering Sciences* **19** (3), 127–132. doi:10.5505/pajes.2013.46855.

Castellarin, A. 2014 Regional prediction of flow-duration curves using a three-dimensional kriging. *Journal of Hydrology* **513**, 179–191. doi:10.1016/j.jhydrol.2014.03.050.

Castellarin, A., Vogel, R. M. & Brath, A. 2004 A stochastic index flow model of flow duration curves. *Water Resources Research* **40**. doi:10.1029/2003WR002524.

Castellarin, A., Camorani, G. & Brath, A. 2007 Predicting annual and long-term flow-duration curves in ungauged basins. *Advances in Water Resources* **30**, 937–953. doi:10.1016/j.advwatres.2006.08.006.

Costa, V., Fernandes, W. & Naghettini, M. 2014 Regional models of flow-duration curves of perennial and intermittent streams and their use for calibrating the parameters of a rainfall–runoff model. *Hydrological Sciences Journal* **59**, 262–277. doi:10.1080/02626667.2013.802093.

Costa, V., Fernandes, W. & Starick, Â. 2020 Identifying regional models for flow duration curves with evolutionary polynomial regression: Application for intermittent streams. *Journal of Hydrologic Engineering* **25**. doi:10.1061/(asce)he.1943-5584.0001873.

de Oliveira, V. A., de Mello, C. R., Viola, M. R. & Srinivasan, R. 2017 Assessment of climate change impacts on streamflow and hydropower potential in the headwater region of the Grande river basin, Southeastern Brazil. *International Journal of Climatology* **37**, 5005–5023. doi:10.1002/joc.5138.

Fearnside, P. M. & Pueyo, S. 2012 Greenhouse-gas emissions from tropical dams. *Nature Climate Change* **2** (6), 382–384. doi:10.1038/nclimate1540.

Franchini, M. & Suppo, M. 1996 Regional analysis of flow duration curves for a limestone region. *Water Resources Management* **10**, 199–218. doi:10.1007/BF00424203.

Fujimura, K., Murakami, M., Iseri, Y. & Kanae, S. 2014 Application of a hydrological model to evaluate the potential hydro energy in a mountainous small river basin of Japan. In: *IAHS-AISH Proceedings and Reports* (Daniell, T., ed.). Copernicus, GmbH, pp. 431–436.

Guiamel, I. A. & Lee, H. S. 2020 Potential hydropower estimation for the Mindanao River Basin in the Philippines based on watershed modelling using the soil and water assessment tool. *Energy Reports* **6**, 1010–1028. doi:10.1016/j.egyr.2020.04.025.

Hashmi, M. Z. & Shamseldin, A. Y. 2014 Use of gene expression programming in regionalization of flow duration curve. *Advances in Water Resources* **68**, 1–12. doi:10.1016/j.advwatres.2014.02.009.

Hu, Z., Liu, S., Zhong, G., Lin, H. & Zhou, Z. 2020 Modified Mann-Kendall trend test for hydrological time series under the scaling hypothesis and its application. *Hydrological Sciences Journal* **65** (14), 2419–2438. doi:10.1080/02626667.2020.1810253.

Huxter, E. H. H. & Van Meerveld, H. J. 2012 Intermittent and perennial streamflow regime characteristics in the Okanagan. *Canadian Water Resources Journal* **37** (4), 391–414. doi:10.4296/cwrj2012-910.

Jung, S., Bae, Y., Kim, J., Joo, H., Kim, H. & Jung, J. 2021 Analysis of small hydropower generation potential: (1) estimation of the potential in ungaged basins. *Energies* **14**. doi:10.3390/en14112977.

Li, M., Shao, Q., Zhang, L. & Chiew, F. H. S. 2010 A new regionalization approach and its application to predict flow duration curve in ungauged basins. *Journal of Hydrology* **389**, 137–145. doi:10.1016/j.jhydrol.2010.05.039.

Mendicino, G. & Senatore, A. 2013 Evaluation of parametric and statistical approaches for the regionalization of flow duration curves in intermittent regimes. *Journal of Hydrology* **480**, 19–32. doi:10.1016/j.jhydrol.2012.12.017.

Mimikou, M. & Kaemaki, S. 1985 Regionalization of flow duration characteristics. *Journal of Hydrology* **82**, 77–91. doi:10.1016/0022-1694(85)90048-4.

Mohor, G. S., Rodriguez, D. A., Tomasella, J. & Siqueira Júnior, J. L. 2015 Exploratory analyses for the assessment of climate change impacts on the energy production in an Amazon run-of-river hydropower plant. *Journal of Hydrology: Regional Studies* **4**, 41–59. doi:10.1016/j.ejrh.2015.04.003.

Moriasi, D. N., Gitau, M. W., Pai, N. & Daggupati, P. 2015 Hydrologic and water quality models: Performance measures and evaluation criteria. *Transactions of the ASABE* **58** (6), 1763–1785. doi:10.13031/trans.58.10715.

Quimpo, R. G., Alejandrino, A. A. & McNally, T. A. 1983 Regionalized flow duration for Philippines. *Journal of Water Resources Planning and Management* **109**, 320–330. doi:10.1061/(asce)0733-9496(1983)109:4(320).

Rianna, M., Efstratiadis, A., Russo, F., Napolitano, F. & Koutsoyiannis, D. 2013 A stochastic index method for calculating annual flow duration curves in intermittent rivers. *Irrigation and Drainage* **62**, 41–49. doi:10.1002/ird.1803.

Rojanamon, P., Chaisomphob, T. & Rattanapitikon, W. 2007 Regional flow duration model for the salawin river basin of Thailand. *ScienceAsia* **33**, 411–419. doi:10.2306/scienceasia1513-1874.2007.33.411.

Rospriandana, N. & Fujii, M. 2017 Assessment of small hydropower potential in the Ciwidey subwatershed, Indonesia: A GIS and hydrological modeling approach. *Hydrological Research Letters* **11**, 6–11. doi:10.3178/hrl.11.6.

Selek, B., Demirel Yazici, D., Aksu, H. & Özdemir, A. D. 2016 Seyhan Dam, Turkey, and climate change adaptation strategies. *Water Resources Development and Management* 205–231. doi:10.1007/978-981-10-1914-2_10.

Shao, Q., Zhang, L., Chen, Y. D. & Singh, V. P. 2009 A new method for modelling flow duration curves and predicting streamflow regimes under altered land-use conditions. *Hydrological Sciences Journal* **54**, 606–622. doi:10.1623/hysj.54.3.606.

Singh, K. P. 1971 Model flow duration and streamflow variability. *Water Resources Research* **7**, 1031–1036. doi:10.1029/WR007i004p01031.

Singh, R. D., Mishra, S. K. & Chowdhary, H. 2001 Regional flow-duration models for large number of ungauged himalayan catchments for planning microhydro projects. *Journal of Hydrologic Engineering* **6**, 310–316. doi:10.1061/(asce)1084-0699(2001)6:4(310).

T.C. Orman ve Su İşleri Bakanlığı 2016 *Antalya Havzası Taşkın Yönetim Planı. Ankara: Su Yönetimi Genel Müdürlüğü (Antalya Basin Flood Management Plan*. Ankara: General Directorate of Water Management 2016.

T.C. Tarım ve Orman Bakanlığı 2018 *Antalya Havzası Kuraklık Yönetim Planı. Ankara: Su Yönetimi Genel Müdürlüğü (Antalya Basin Drought Management Plan*. Ankara: General Directorate of Water Management 2018).

Thin, K. K., Zin, W. W., San, Z. M. L. T., Kawasaki, A., Moiz, A. & Bhagabati, S. S. 2020 Estimation of run-of-river hydropower potential in the myitnge river basin. *Journal of Disaster Research* **15**, 267–276. doi:10.20965/jdr.2020.p0267.

Tramblay, Y., Koutroulis, A., Samaniego, L., Vicente-Serrano, S. M., Volaire, F., Boone, A., Page, M. L., Llasat, M. C., Albergel, C., Burak, S., Cailleret, M., Cindrić, K., Davi, H., Dupuy, J.-L., Greve, P., Grillakis, M., Hanich, L., Jarlan, L., Martin-StPaul, N., Martínez-Vilalta, J., Mouillot, F., Pulido-Velazquez, D., Quintana-Seguí, P., Renard, D., Turco, M., Türkeş, M., Trigo, R., Vidal, J.-P., Vilagrosa, A., Zribi, M. & Polcher, J. 2020 Challenges for drought assessment in the Mediterranean region under future climate scenarios. *Earth-Science Reviews* **210**, 103348. doi:10.1016/j.earscirev.2020.103348.

Vaheddoost, B., Yilmaz, M. U. & Safari, M. J. S. 2023 Estimation of flow duration and mass flow curves in ungauged tributary streams. *Journal of Cleaner Production* **409**. doi:10.1016/j.jclepro.2023.137246.

Valero, E. 2012 Characterization of the water quality status on a stretch of River Lérez around a small hydroelectric power station. *Water* **4** (4), 815–834. doi:10.3390/w4040815.

Yankey, B. E., Gyamfi, C., Arthur, E., Dekongmen, B. W., Asantewaa-Tannor, P., Tawiah, J. K. & Mends, L. G. 2023 Small hydropower development potential in the Densu River Basin, Ghana. *Journal of Hydrology: Regional Studies* **45**. doi:10.1016/j.ejrh.2022.101304.

Yilmaz, K. K., Gupta, H. V. & Wagener, T. 2008 A process-based diagnostic approach to model evaluation: Application to the NWS distributed hydrologic model. *Water Resources Research* **44** (9), W09417. doi:10.1029/2007WR006716.

Yilmaz, M. U., Aksu, H., Onoz, B. & Selek, B. 2023 An effective framework for improving performance of daily streamflow estimation using statistical methods coupled with artificial neural network. *Pure and Applied Geophysics* **180** (10), 3639–3654. doi:10.1007/s00024-023-03344-5.

Yu, P.-S., Yang, T.-C. & Wang, Y.-C. 2002 Uncertainty analysis of regional flow duration curves. *Journal of Water Resources Planning and Management* **128**, 424–430. doi:10.1061/(asce)0733-9496(2002)128:6(424).

Yuksel, I. 2010 Hydropower for sustainable water and energy development. *Renewable & Sustainable Energy Reviews* **14** (1), 462–469. doi:10.1016/j.rser.2009.07.025.

Ziv, G., Baran, E., Nam, S., Rodríguez-Iturbe, I. & Levin, S. A. 2012 Trading-off fish biodiversity, food security, and hydropower in the Mekong River Basin. *Proceedings of the National Academy of Sciences of the United States of America* **109** (15), 5609–5614. doi:10.1073/pnas.1201423109.

First received 10 March 2024; accepted in revised form 30 July 2024. Available online 13 August 2024